Dissipative quantum dynamics in low-energy collisions of complex nuclei

A. Diaz-Torres, D. J. Hinde, and M. Dasgupta
Department of Nuclear Physics, Research School of Physical Sciences and Engineering
Australian National University, Canberra, ACT 0200, Australia

G. J. Milburn
Centre for Quantum Computer Technology, University of Queensland, St. Lucia, Queensland 4072, Australia

J. A. Tostevin
Department of Physics, Faculty of Engineering and Physical Sciences, University of Surrey, Guildford, Surrey GU2 7XH, United Kingdom
(Received 14 February 2008; revised manuscript received 23 October 2008; published 5 December 2008)

Model calculations that include the effects of irreversible, environmental couplings on top of a coupled-channels dynamical description of the collision of two complex nuclei are presented. The Liouville-von Neumann equation for the time evolution of the density matrix of a dissipative system is solved numerically providing a consistent transition from coherent to decoherent (and dissipative) dynamics during the collision. Quantum decoherence and dissipation are clearly manifested in the model calculations. Energy dissipation, due to the irreversible decay of giant-dipole vibrational states of the colliding nuclei, is shown to result in a hindrance of quantum tunneling and fusion.

DOI: 10.1103/PhysRevC.78.064604 PACS number(s): 25.70.Jj, 03.65.Yz, 24.10.Eq, 25.60.Pj

I. INTRODUCTION

Collisions of composite nuclei involve a complicated interplay and exchange of energy and angular momentum between the relative motion and the intrinsic states of the nuclei. High precision data for low-energy fusion reactions provide one of the most sensitive tests of such interplay. Stationary state coupled-channels descriptions have provided a natural methodology to study the effects of specific excitation modes of one or both of the reactants on the reaction outcomes. The wave function in this Schrödinger coupled-channels picture is a linear superposition of the states in the model space with a definite phase relationship. This coherent linear superposition can result in enhancement of the quantum tunneling probability and quantum interference. The coupled-channels approach has been very successful [1] in explaining several collision observables. However, problems remain. Foremost is the inability to describe elastic scattering and fusion measurements simultaneously [2,3] and, related, the more recent failure to describe in a physically consistent way the below-barrier quantum tunneling and above-barrier fusion yields [4].

The coupled-channels treatment of collisions of complex nuclei as closed quantum systems is an approximation. In practice, collisions evolve as open quantum systems, with innumerable bound and continuum intrinsic excitations of the nuclei. In analogy with problems of a quantum system in a bath, and following Bohr and Mottelson [5], we view the nuclear many-body Hamiltonian as a sum of collective, single-particle, and coupling terms. In a nuclear collision, the collective part comprises the relative motion of the nuclei and intrinsic rotational and/or vibrational modes. Only a fraction of the Hilbert space of this Hamiltonian is used in *any* feasible full coupled-channels calculation. This is because the model space is inevitably restricted to selected, most collective intrinsic excitations. These collective states define a *reduced* quantum system. All other states are *weakly* coupled to this reduced system by residual interactions and constitute an "environment." The key question that arises is: do environmental effects influence the reaction dynamics and observables, such as angular distributions of products or tunneling rates?

In modeling fusion, the environment is assumed to come into play only inside the fusion barrier and is accounted for in coupled-channels calculations through an imaginary potential or an ingoing wave boundary condition. However, environmental effects can also be manifested before the nuclei encounter the fusion barrier, for example, as real or virtual excitations of giant resonances in the individual nuclei by the long-range Coulomb excitation mechanism. These can be important doorway states to the irreversible loss of kinetic energy (heating of the nuclei), as first suggested in Ref. [6] for deep-inelastic reactions. Another mechanism is complicated multinucleon transfer channels [7]. Measurements have shown that deep-inelastic processes occur even at subbarrier incident energies [8], in competition with the process of quantum tunneling, and thus fusion [9]. Energy loss associated with the deep-inelastic mechanism thus could play a significant role in the inhibition of tunneling at deep subbarrier energies.

The investigation of the effect, on near- and below-barrier fusion, here requires a dynamical model that can include both intrinsic state and environmental couplings in calculations of the tunneling probability. There are no existing realistic theoretical approaches for solving this problem. Within a model context, this article (1) discusses how environment-induced irreversibility can be incorporated into the successful coupled-channels framework and (2) makes a first assessment of its effect on a low-energy nuclear collision. The application considered is quantum tunneling, relevant to the low-energy nuclear fusion hindrance phenomenon.

The article is organized as follows. In Sec. II we give a brief survey of theoretical approaches to dissipative dynamics of low-energy nuclear collisions and discuss the suitability of the Lindblad axiomatic theory for the treatment of energy dissipation on subbarrier fusion. In Sec. III we present the coupled-channels density matrix approach. Numerical results for our model test case are discussed in Sec. IV. Finally, the summary of the article is given in Sec. V.

II. THEORETICAL BACKGROUND

Neither existing models of fusion nor of deep-inelastic scattering can address both energy dissipation and quantum tunneling. The impact of finite lifetimes of excited states (e.g., giant resonances) on fusion has been studied within a coupled-channels model [10–12], but this approach does not lead to energy dissipation. Direct damped collisions between complex nuclei have also been intensively investigated within various approaches, including (i) transport theories [13] based on premaster, master, Fokker-Planck, Langevin, and diffusion equations and (ii) quantum mechanical collective theories [14]. An appealing semiclassical coupled-channels approach combined with a random-matrix model has been suggested by Ko [15], which unifies the statistical and coherent pictures of energy dissipation in deep-inelastic collisions. This framework has been successfully applied [16,17] to study the excitation of multiphonon giant resonances in heavy-ion collisions at intermediate energy. In most of these developments the relative motion of the nuclei is described with classical trajectories, while the coupling to intrinsic degrees of freedom is treated either statistically (random-matrix theory) or through phenomenological transport coefficients. However, the quantum mechanical treatment of the relative motion is essential for dealing with quantum tunneling.

The quantum dynamical model presented in this work is based on the time evolution of a reduced density matrix. It provides a consistent description of the transition from a pure state to a mixed quantum state during the collision. The fundamental equation of motion is the Liouville-von Neumann equation for an open quantum system, in which a dissipative Liouvillian accounts for irreversibility due to interactions of the system with an environment. The Lindblad axiomatic approach [18,19] for open quantum systems has been successfully applied in nuclear physics, but within rather schematic models. For instance, to describe the charge equilibration process in deep-inelastic collisions [20], fission [21], decay of giant resonances [22], tunneling through a parabolic barrier [23], and scattering in a two-dimensional inverse parabolic potential [24]. These are calculations for a *single* channel of either one damped oscillator [21–23] or two coupled damped oscillators [20,24].

In low-energy nuclear collisions, the context of the present application, Lindblad's dynamics for the evolution of the reduced system is justified (i) because the coupling to the complex environment (through excited doorway states and determined by residual interactions) is weak and (ii) because the Markov approximation is expected to be valid, the collective motions of the two nuclei being slower than the rearrangement of the environmental (nucleonic) degrees of freedom. With increasing collision energy, to well above the Coulomb barrier, memory effects related to diabatic dynamics [25–27] may be important and a non-Markovian Liouvillian may be required. The weak coupling between two subspaces of the total space of intrinsic nuclear states distinguishes between the system and the environment. The Lindblad theory does not require [28] any limitation on the strength of the system-environment coupling, although the definition of physically well-defined environment states would require a careful analysis in the strong-coupling limit.

An essential effect of the environment on the reaction dynamics (unlike the effect of absorptive terms) is to progressively destroy the coherent linear superposition and the associated phase relationships between different channels, introducing quantum decoherence in the system.

Here, we identify two such (model) sources of decoherence and dissipation. First, an environment inside the Coulomb barrier, which is related to the complexity of compound nucleus states. Second, one with effectively a long range, associated with decay out of short-lived (compared to the reaction time) internal vibrational states, e.g., the giant dipole resonance (GDR) of the colliding nuclei, will be shown to be of particular importance. The damping of the GDR, because of its irreversible coupling to a sea of complicated surrounding states, which constitute the environment [29], destroys the coherent dynamical coupling with the relative motion of the nuclei. Here we show that damping of the GDR results in decoherence and energy loss in the region where the nuclei overlap, inhibiting tunneling and thus fusion.

III. COUPLED-CHANNELS DENSITY MATRIX APPROACH

We exploit the time evolution of a coupled-channels density matrix, as is employed in quantum molecular dynamics [30]. The density operator $\hat{\rho}$ in Eq. (1) is represented in an asymptotic (product) basis of states of the internal Hamiltonian of the individual nuclei, $|i\rangle$, $i = 1, \ldots, N$ (lower indices), and coordinate states describing the separation of the two nuclei, $|r)$, $r = 1, \ldots, M$ (upper indices). That is,

$$\hat{\rho} = \sum_{ij,rs} |r)|i\rangle \rho_{ij}^{rs} \langle j|(s|. \tag{1}$$

Crucially, we also add two auxiliary states to the $|i\rangle$ basis that allow distinct environmental interactions, as described below. The density operator obeys the time-dependent Liouville-von Neumann equation

$$\frac{\partial \hat{\rho}}{\partial t} = \hat{\mathcal{L}}\hat{\rho} = [\hat{\mathcal{L}}_H + \hat{\mathcal{L}}_D]\hat{\rho}, \tag{2}$$

where the total Liouvillian consists of a Hamiltonian part $\hat{\mathcal{L}}_H\hat{\rho} = -i[\hat{H}, \hat{\rho}]/\hbar$ describing the coherent evolution of the system with Hamiltonian $\hat{H}$ and a dissipative part $\hat{\mathcal{L}}_D$ accounting for the interactions with the environment. Here, $\hat{\mathcal{L}}_D$ is assumed to be given by Lindblad's dissipative Liouvillian

[18,19] associated with a Markovian semigroup evolution, i.e.,

$$\hat{\mathcal{L}}_D\hat{\rho} = \sum_\alpha \left(\hat{\mathcal{C}}_\alpha\hat{\rho}\hat{\mathcal{C}}_\alpha^\dagger - \frac{1}{2}[\hat{\mathcal{C}}_\alpha^\dagger\hat{\mathcal{C}}_\alpha, \hat{\rho}]_+\right), \tag{3}$$

where $[\ldots]_+$ denotes the anticommutator. Here each $\hat{\mathcal{C}}_\alpha$ is a Lindblad operator for a dissipative coupling, physically motivated according to the specific problem. We assume that each coupling $\alpha \equiv (Ij)$ between a given state $|j\rangle$ and an environmental state $|I\rangle$ has an associated rate Γ_{Ij}, i.e, $\hat{\mathcal{C}}_{Ij} = \sqrt{\Gamma_{Ij}}|I\rangle\langle j|$ [31], determined by the inverse lifetime of the excited states and the branching ratio of its deexcitation, taken to be that when the nuclei are well separated. We note also that (a) the Lindblad Liouvillian has been derived using microscopic models [22,32] and (b), in contrast to many (dissipative) model Liouvillians [19], Eq. (3) preserves both the positivity and the trace of the density matrix. These are essential properties in any realistic application.

In the model calculations that follow, the basis comprises two asymptotic states (coupled-channels) $|1\rangle$ and $|2\rangle$ with channel energies e_j. Channel $|1\rangle$ is the (ground states) entrance channel and is coupled to an inelastic state $|2\rangle$ by a coupling interaction V_{12}. Two distinct sources of irreversibility are also considered, modeled by two auxiliary (environment) states $|X\rangle$ and $|Y\rangle$. The first environmental coupling describes capture by the potential pocket inside the fusion barrier. This simulates the irreversible and dissipative excitations associated with the evolution from the two separate nuclei to a compound nuclear system. In a stationary states approach this loss of flux is approximated by imposing an imaginary potential $-iW(r)$, $W(r) > 0$, or an ingoing wave boundary condition at distances well inside the barrier. Here, these transitions are described by an auxiliary state $|X\rangle$, to which *all* other states $|j\rangle$ couple, modeled [33] by a Lindblad operator, $\hat{\mathcal{C}}_{Xj} = \sqrt{\gamma^{rr}}|X\rangle\langle j|$. The absorption rate to state $|X\rangle$ is given by $\gamma^{rr} = W(r)/\hbar$, where $W(r)$ is taken as a Fermi function with depth 10 MeV and diffuseness 0.1 fm, located at the pocket radius of the nucleus-nucleus potential, $\approx$7 fm. This choice guarantees complete absorption inside the pocket. The fusion probability is defined as the probability accumulating in this state $|X\rangle$.

The second environment, whose explicit treatment will be seen to be the most significant at lower energies, is associated with the irreversible decay out of intrinsic excitations of the colliding nuclei. Such decays are independent of the dynamical couplings. Specifically, we associate the ONLY excited coupled-channel state $|2\rangle$ with the GDR excitation. We then introduce a second auxiliary state $|Y\rangle$, representing the bath of states in which the GDR is embedded and to which only the GDR excitation $|2\rangle$ is coupled.

Thus, $|Y\rangle$ and/or $|X\rangle$ supplement the two intrinsic states $|1\rangle$ and $|2\rangle$ that compose the two coupled channels. Both of the auxiliary states refer to complex excitation modes of the nuclei, associated with nucleonic degrees of freedom and compound nucleus states, respectively. They provide intuitive and formal channels [33] for describing irreversible coupling and loss of probability from the system to these environments, couplings that enter *only* through the dissipative dynamics term $\hat{\mathcal{L}}_D$ in Eq. (2). $|Y\rangle$ is also assumed to couple to $|X\rangle$ at the appropriate

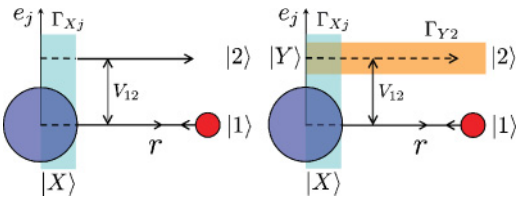

FIG. 1. (Color online) Schematic representations of the dissipative coupled channels model calculations, with channel energies e_j, showing the spatial and energy localization of the auxiliary (environment) states $|X\rangle$ and $|Y\rangle$ (shaded rectangles). The left-hand panel shows the dynamical calculation scheme in the presence of environment $|X\rangle$ only. The right-hand panel shows the dynamical calculation scheme in the presence of both environments $|X\rangle$ and $|Y\rangle$. Here, dashed lines indicate regions where the intrinsic channels $|1\rangle$ and $|2\rangle$ experience irreversible couplings to the environmental states $|X\rangle$ and/or $|Y\rangle$.

range of separations. Probability accumulating in state $|Y\rangle$ outside of this $|X\rangle$ pocket may be identified with deep-inelastic processes, as is discussed later. These environments and the couplings present in the model calculations are represented schematically in Fig. 1. There, dashed lines indicate regions where the intrinsic coupled-channels states $|1\rangle$ and $|2\rangle$ experience irreversible (environment) couplings to states $|X\rangle$ and/or $|Y\rangle$.

Upon inserting Eq. (1) into Eq. (2), the following coupled equations are obtained for the time evolution of the density matrix elements,

$$\dot{\rho}_{ij}^{rs} = (\hat{\mathcal{L}}_H\hat{\rho})_{ij}^{rs} + (\hat{\mathcal{L}}_D\hat{\rho})_{ij}^{rs}. \tag{4}$$

Explicitly, the Hamiltonian terms are given by

$$(\hat{\mathcal{L}}_H\hat{\rho})_{ij}^{rs} = -\frac{i}{\hbar}\left[\rho_{ij}^{rs}(e_i - e_j) + \sum_{t=1}^{M}(T^{rt}\rho_{ij}^{ts} - \rho_{ij}^{rt}T^{ts}) + \rho_{ij}^{rs}(U^{rr} - U^{ss}) + \sum_{k=1}^{N}(V_{ik}^{rr}\rho_{kj}^{rs} - \rho_{ik}^{rs}V_{kj}^{ss})\right], \tag{5}$$

where i, j, and k run only over intrinsic states $|1\rangle, |2\rangle, \ldots$. The dissipative terms are given by

$$(\hat{\mathcal{L}}_D\hat{\rho})_{ij}^{rs} = \delta_{ij}\sum_k \tilde{\Gamma}_{ik}^{rr}\rho_{kk}^{rs} - \frac{1}{2}\left[\sum_k(\tilde{\Gamma}_{ki}^{rr} + \tilde{\Gamma}_{kj}^{rr})\right]\rho_{ij}^{rs}, \tag{6}$$

where the indices run over all the included intrinsic state to auxiliary state couplings and $\tilde{\Gamma}_{ij}^{rr} = \Gamma_{ij} + \gamma^{rr}$. In Eq. (5), T, U, and V refer to the relative kinetic energy, the total bare nucleus-nucleus potential (Coulomb + nuclear), and the coupling interaction between the intrinsic channels, respectively.

While not the technique that is used here, we note that this Lindblad dynamical model can also be recast and solved numerically within the Monte Carlo wave function method (see, e.g., Ref. [34]). In that approach, decoherence and dissipation originate from the introduction of random quantum jumps in the time evolution of the wave function of the system. This unraveling density matrix evolution, through stochastic wave function methods [34], shows that the two approaches are equivalent and the former takes into account the role of

fluctuations in the calculation of the expectation values and variances of observables.

The present calculational scheme is based on Eqs. (5) and (6) and proceeds as follows. Initially, at time $t = 0$, the nuclei are well separated in their ground states, and their density matrix describes a pure state with $\mathrm{Tr}[\hat{\rho}] = \mathrm{Tr}[\hat{\rho}^2] = 1$. An initial wave-packet describes the relative motion of the nuclei. The coupled equations are solved numerically using the Faber polynomial expansion of the time evolution superoperator [35], $\exp(\tau\hat{\mathcal{L}})$, and the Fourier method of Ref. [36] for the commutator between the kinetic energy and density operator. Having solved for the dynamical evolution of the density matrix, expectation values of an observable $\hat{\mathcal{O}}$ are now obtained from the trace relation $\langle\hat{\mathcal{O}}(t)\rangle = \mathrm{Tr}[\hat{\mathcal{O}}\hat{\rho}(t)]$. The purity of the initial state, conserved under Hamiltonian unitary evolution, will be destroyed ($\mathrm{Tr}[\hat{\rho}^2] < 1$) if the environment causes a loss of quantum coherence. This decoherence can thus be quantified via this loss of density matrix purity, or equivalently by an increase of the linear entropy $1 - \mathrm{Tr}[\hat{\rho}^2]$.

IV. NUMERICAL RESULTS AND DISCUSSION

So as to make contact with the coherent Schrödinger picture, the model Hamiltonian we used was chosen to coincide with that of the coupled-channels fusion model CCFULL [37]. Specifically, our model calculations use physical parameters relevant to the $^{16}\mathrm{O} + ^{144}\mathrm{Sm}$ reaction at collision energies below its nominal fusion barrier, $V_B = 61.1$ MeV. We assume zero relative orbital angular momentum between the reactants. The form of the bare nuclear potential between the two nuclei, consistent with the stated V_B, is a Woods-Saxon potential with $(V_0, r_0, a_0) \equiv (-105.1$ MeV, 1.1 fm, 0.75 fm). The Coulomb potential was that for two point charges. The ^{16}O projectile was taken to be inert and the ^{144}Sm target was allowed to be excited to a GDR vibrational state. The dynamical nuclear coupling of the ground state $|1\rangle$ to the vibrational state $|2\rangle$, with excitation energy $E_{1^-} = 15$ MeV, has a macroscopic deformed Woods-Saxon form with a deformation parameter of $\beta_1 = 0.2$.

The time step for the density matrix propagation was $\Delta t = 10^{-22}$ s, and the radial grid ($r = 0$–250 fm) was evenly spaced with $M = 512$ points. The relative motion of the two nuclei in the entrance channel $|1\rangle$ was described by a minimal-uncertainty Gaussian wave packet, with width $\sigma_0 = 20$ fm, initially centered at $r = 150$ fm, and was boosted toward the target with the appropriate average kinetic energy for the entrance channel energy E_0 required. The FWHM energy spread of the wave packet was ~3%. The numerical accuracy of the time evolution was checked using a fully coherent, time-dependent calculation, excluding coupling to states $|X\rangle$ and $|Y\rangle$. It was confirmed that the normalization and purity of the density matrix, $\mathrm{Tr}[\hat{\rho}] = \mathrm{Tr}[\hat{\rho}^2] = 1$, and the expectation value of the system energy $\mathrm{Tr}[\hat{H}\hat{\rho}]$ were maintained with high accuracy over the required number of time steps, typically 700 for the full duration of the collision.

TABLE I. The calculated density matrix purity $\mathrm{Tr}[\hat{\rho}^2]$ and energy loss $\Delta E = \mathrm{Tr}[\hat{\mathrm{H}}(\hat{\rho}_0 - \hat{\rho})]$ following time evolution (for 700 time steps) when including only the state $|X\rangle$ and both states $|X\rangle$ and $|Y\rangle$ environmental couplings. The GDR coupling strength used was $\beta_1 = 0.2$.

E_0 (MeV)	State $\|X\rangle$		States $\|X\rangle$ and $\|Y\rangle$	
	$\mathrm{Tr}[\hat{\rho}^2]$	ΔE (MeV)	$\mathrm{Tr}[\hat{\rho}^2]$	ΔE (MeV)
45	1.0000	0.0004	0.9196	1.8718
50	1.0000	0.0004	0.8977	2.6744
55	0.9996	0.0109	0.8759	3.6100
60	0.6067	14.862	0.5127	18.908

The importance of the two, spatially distinct, sources of environment couplings was studied. Calculations were first performed in the scheme shown in the left panel of Fig. 1. Here the intrinsic coupled channels $|1\rangle$ and $|2\rangle$ also couple to the capture state $|X\rangle$. Calculations were carried out for $E_0 = 45$, 50, 55, and 60 MeV incident energy. The calculated state purity $\mathrm{Tr}[\hat{\rho}^2]$ and the energy dissipation $\mathrm{Tr}[\hat{H}(\hat{\rho}_0 - \hat{\rho})]$ post the collision (after 700 time steps) are shown in the left-hand columns in Table I. For sufficiently subbarrier energies, $E_0 \leqslant 55$ MeV, it is evident that time evolution in the presence of state $|X\rangle$ essentially maintains coherence and is nondissipative. There is, however, loss of purity and dissipation at the highest energy. It is interesting, therefore, to compare the density matrix and the Schrödinger predictions of CCFULL (that uses an ingoing wave boundary condition). This is done here only for calculations of the tunneling probability $P(E_0)$, in a relative s wave, shown in Fig. 2(a). These comparisons, of necessity, require convolution of the $\ell = 0$ partial wave penetrabilities $T_0(E)$ from CCFULL with

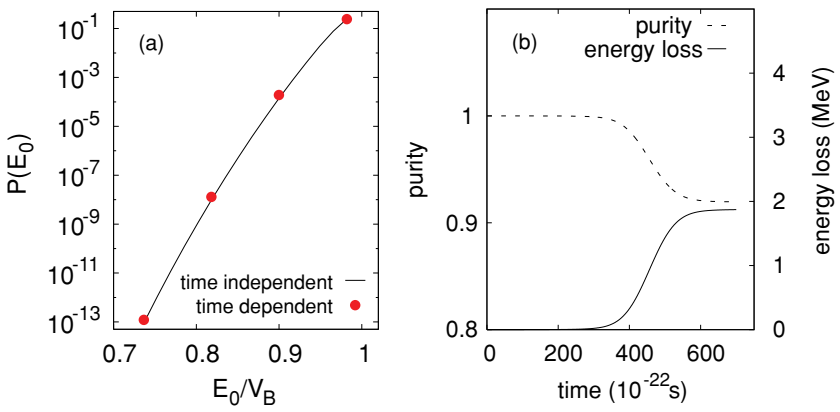

FIG. 2. (Color online) (a) The energy dependence of the s-wave tunneling probability calculated with the density matrix (solid points) and the coupled-channels CCFULL methods (solid line). (b) The time evolution of the density matrix purity $\mathrm{Tr}[\hat{\rho}^2]$ and the energy loss $\mathrm{Tr}[\hat{H}(\hat{\rho}_0 - \hat{\rho})]$ with decoherent $|X\rangle$ and $|Y\rangle$ state dynamics, corresponding to the right-hand $E_0 = 45$ MeV entry in Table I.

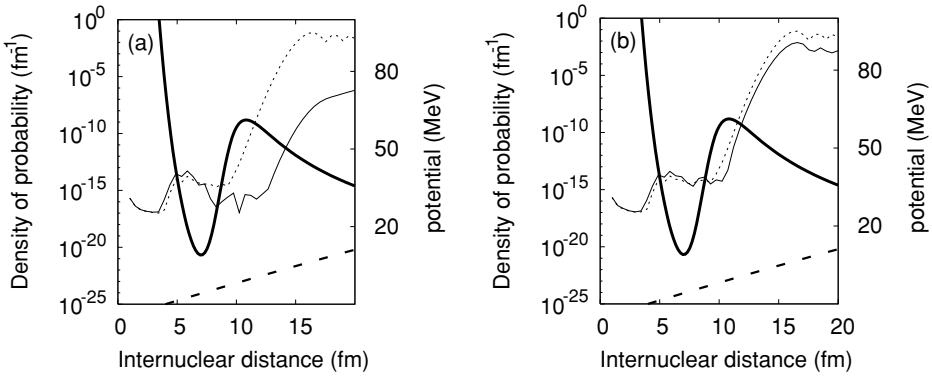

FIG. 3. The internuclear potential (thick curve) and the time evolution of the wave packet for $^{16}O + ^{144}Sm$ at $E_0 = 45$ MeV: (a) including only coupling of the auxiliary state $|X\rangle$, (b) including coupling of the states $|X\rangle$ and $|Y\rangle$. The wave packet is plotted at times $t = 0$ (dashed curve), 400×10^{-22} s (dotted curve), and 700×10^{-22} s (thin solid curve).

the energy distribution $f(E, E_0)$ of the chosen initial wave packet. That is, $P(E_0) \equiv \int dE\, f(E, E_0) T_0(E)$. The $P(E_0)$, shown as a function of E_0/V_B in Fig. 2(a), are in very good agreement showing the appropriateness of stationary state coupled-channels calculations for this observable within the dynamical scheme of states $|1\rangle$, $|2\rangle$, and $|X\rangle$. It is our contention that the dissipation associated with state $|X\rangle$, while significant at 60 MeV, is strongly localized inside the barrier and thus does not impact upon the barrier penetrability. We will now show that the same is not true for the more spatially extended dissipation due to the GDR decay environment $|Y\rangle$.

The treatment of the irreversible GDR decay (with a spreading width of 6 MeV) to the bath of surrounding complex states (represented by $|Y\rangle$) was included by switching on the coupling of the intrinsic inelastic state $|2\rangle$ to $|Y\rangle$. This is the dynamical scheme of the right-hand panel in Fig. 1. Unlike the coupling to $|X\rangle$, a major part of the inelastic excitation of the system gives access to $|Y\rangle$ before the wave packet encounters the fusion barrier. The onset of decoherence, the purity of the density matrix, and the associated energy dissipation are shown in the right-hand entries in Table I and, as a function of time evolution, in Fig. 2(b), the latter for $E_0 = 45$ MeV.

Summing over all internal states of the density matrix gives the total diagonal elements in coordinate space, which represent the wave packet at a given time. Snapshots of the wave packet in the interaction region (for $E_0 = 45$ MeV) are shown in Fig. 3. The curves are shown for times $t = 0$ (dashed, the initial state), 400×10^{-22} s (dotted, near to the time of closest approach), and 700×10^{-22} s (thin solid, post the collision). Figure 3 shows the results from (a) the coupling to state $|X\rangle$ and (b) to both $|X\rangle$ and $|Y\rangle$. When the wave packet tunnels into the pocket (from dashed to dotted lines), the short-range coupling to $|X\rangle$ leads to trapping of flux from $|1\rangle$ and $|2\rangle$ inside the potential pocket. This reveals itself as an unchanging probability for radii $r < 7.5$ fm as the main body of the wave packet leaves the interaction region (from the dotted to the thin solid lines) in Fig. 3(a). The additional effect of turning on the coupling between states $|2\rangle$ and $|Y\rangle$ is to trap probability *under* the barrier, as is shown in Fig. 3(b). This reduces the component of the wave packet that reaches the potential pocket, inhibiting the quantum tunneling.

The probability trapped under the fusion barrier is associated with GDR collective vibrational energy being irreversibly removed from the coherent dynamics into innumerable channels (heat). This is then no longer available for relative motion, or tunneling. Such energy loss can be correlated with deep-inelastic processes, seen experimentally, that compete with fusion in reactions involving heavy nuclei [8].

Figure 4(a) shows the time evolution of the probability trapped in the potential pocket, state $|X\rangle$, for $E_0 = 45$ MeV. We comment that, when including the inelastic channel $|2\rangle$ but not $|Y\rangle$, the nucleus-nucleus potential renormalization leads to the expected enhanced penetrability from the inelastic channel coupling, compared to the purely elastic ($|1\rangle$ plus $|X\rangle$) calculation. The decoherent dynamics due only to environment $|X\rangle$ gives the (full curve). By comparison, the calculation that also includes the GDR doorway-state decay to $|Y\rangle$ leads to a

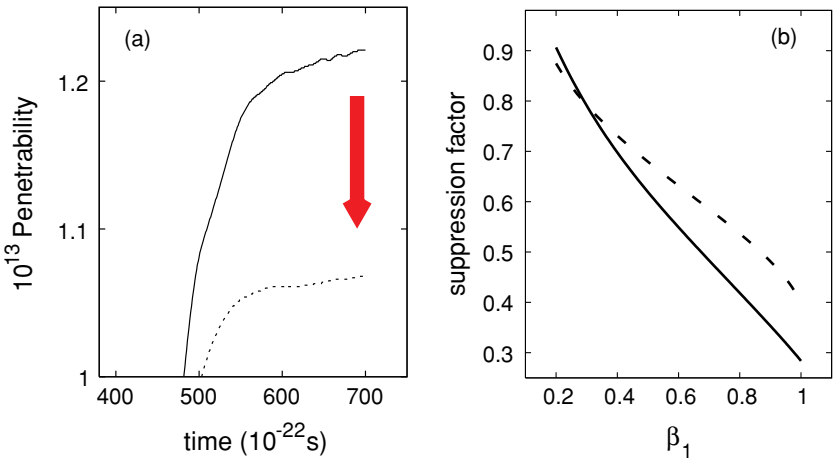

FIG. 4. (Color online) (a) Time dependence of the probability trapped in $|X\rangle$ for $E_0 = 45$ MeV. The full curve includes states $|1\rangle$, $|2\rangle$, and $|X\rangle$. The dotted curve adds the irreversible decay of $|2\rangle$ to $|Y\rangle$. The calculations are for $\beta_1 = 0.2$. (b) Calculated suppression of the probability trapped in $|X\rangle$ as a function of the assumed β_1 value for $E_0 = 45$ MeV (dashed curve) and 55 MeV (solid curve).

suppression (dotted curve and arrow) of the population of state $|X\rangle$. Additional irreversible processes other than excitation of the GDR are also likely to contribute to the deep-inelastic yield, such as complicated multinucleon transfers [7]. To simulate these very simply, the assumed state $|1\rangle$ to $|2\rangle$ coupling strength was increased. Figure 4(b) shows the dependence of the calculated tunneling suppression on the assumed β_1 strength for $E_0 = 45$ (dashed curve) and 55 MeV (solid curve), where we note that larger β_1 values result in both an increase in the strength and the range of the coupling form factor to the inelastic state $|2\rangle$.

V. SUMMARY

A quantum dynamical model based on time propagation of a coupled-channels density matrix has been presented and is shown to describe the transition from pure state (coherent) to mixed state (decoherent and dissipative) dynamics during a nuclear collision. The calculations exhibit both decoherence and energy dissipation and so go beyond coherent coupled-channels approaches. Decoherence, originating here from the irreversible decay of a giant-dipole vibrational state of the heavy target nucleus to surrounding states, is shown to result in hindrance of quantum tunneling. Developments of the model calculations to include (a) nonzero relative orbital angular momenta between the reactants, (b) additional intrinsic channels, and (c) a more detailed consideration of other processes, such as multinucleon or cluster transfer reactions, are necessary to confront experimental measurements.

ACKNOWLEDGMENTS

We thank J. O. Newton and L. R. Gasques for constructive suggestions. Support from an ARC Discovery grant and UK Science and Technology Facilities Council (STFC) Grant EP/D003628/1 is acknowledged.

[1] I. J. Thompson, Comput. Phys. Rep. **7**, 167 (1988).
[2] J. O. Newton *et al.*, Phys. Lett. **B586**, 219 (2004).
[3] A. Mukherjee, D. J. Hinde, M. Dasgupta, K. Hagino, J. O. Newton, and R. D. Butt, Phys. Rev. C **75**, 044608 (2007).
[4] M. Dasgupta, D. J. Hinde, A. Diaz-Torres, B. Bouriquet, C. I. Low, G. J. Milburn, and J. O. Newton, Phys. Rev. Lett. **99**, 192701 (2007), and references therein.
[5] A. Bohr and B. R. Mottelson, *Nuclear Structure* (Benjamin, New York, 1975), Vol. 2.
[6] R. A. Broglia, C. H. Dasso, and A. Winther, Phys. Lett. **B61**, 113 (1976).
[7] K. E. Rehm, Annu. Rev. Nucl. Part. Sci. **41**, 429 (1991).
[8] F. L. H. Wolfs, Phys. Rev. C **36**, 1379 (1987).
[9] C. H. Dasso and G. Pollarolo, Phys. Rev. C **39**, 2073 (1989).
[10] M. S. Hussein and A. F. R. de Toledo Piza, Phys. Rev. Lett. **72**, 2693 (1994).
[11] M. S. Hussein, M. P. Pato, and A. F. R. de Toledo Piza, Phys. Rev. C **51**, 846 (1995).
[12] K. Hagino and N. Takigawa, Phys. Rev. C **58**, 2872 (1998).
[13] W. U. Schröder and J. R. Huizenga, *Treatise on Heavy-Ion Science*, edited by D. A. Bromley (Plenum, New York, 1984), Vol. 2, p. 140, and references therein.
[14] J. A. Maruhn, W. Greiner, and W. Scheid, *Heavy Ion Collisions*, edited by R. Bock (North-Holland, Amsterdam, 1980), Vol. 2, p. 127, and references therein.
[15] C. M. Ko, Z. Phys. A **286**, 405 (1978).
[16] B. V. Carlson, M. S. Hussein, A. F. R. de Toledo Piza, and L. F. Canto, Phys. Rev. C **60**, 014604 (1999).
[17] M. S. Hussein, B. V. Carlson, and L. F. Canto, Nucl. Phys. **A731**, 163 (2004).
[18] G. Lindblad, Commun. Math. Phys. **48**, 119 (1976).
[19] A. Sandulescu and H. Scutaru, Ann. Phys. (NY) **173**, 277 (1987).
[20] A. Sandulescu, H. Scutaru, and W. Scheid, J. Phys. A **20**, 2121 (1987).
[21] E. Stefanescu, W. Scheid, A. Sandulescu, and W. Greiner, Phys. Rev. C **53**, 3014 (1996).
[22] E. Stefanescu, R. J. Liotta, and A. Sandulescu, Phys. Rev. C **57**, 798 (1998).
[23] G. G. Adamian, N. V. Antonenko, and W. Scheid, Nucl. Phys. **A645**, 376 (1999).
[24] M. Genkin and W. Scheid, J. Phys. G **34**, 441 (2007).
[25] W. Nörenberg, Phys. Lett. **B104**, 107 (1981).
[26] A. Diaz-Torres and W. Scheid, Nucl. Phys. **A757**, 373 (2005).
[27] A. Diaz-Torres, Phys. Rev. C **69**, 021603(R) (2004); **74**, 064601 (2006).
[28] K. Dietz, J. Phys. A **37**, 6143 (2004).
[29] G. F. Bertsch, P. F. Bortignon, and R. A. Broglia, Rev. Mod. Phys. **55**, 287 (1983).
[30] L. Pesce and P. Saalfrank, J. Chem. Phys. **108**, 3045 (1998).
[31] C. Scheurer and P. Saalfrank, J. Chem. Phys. **104**, 2869 (1996).
[32] S. Gao, Phys. Rev. B **57**, 4509 (1998); O. Linden *et al.*, Eur. Phys. J. D **12**, 473 (2000); Z. Kanokov, Y. V. Palchikov, G. G. Adamian, N. V. Antonenko, and W. Scheid, Phys. Rev. E **71**, 016121 (2005); D. Lacroix, Phys. Rev. C **73**, 044311 (2006).
[33] I. Burghardt, J. Phys. Chem. A **102**, 4192 (1998).
[34] K. Mølmer, Y. Castin, and J. Dalibard, J. Opt. Soc. Am. B **10**, 524 (1993).
[35] W. Huisinga, L. Pesce, R. Kosloff, and P. Saalfrank, J. Chem. Phys. **110**, 5538 (1999).
[36] R. Kosloff, Annu. Rev. Phys. Chem. **45**, 145 (1994).
[37] K. Hagino, N. Rowley, and A. T. Kruppa, Comput. Phys. Commun. **123**, 143 (1999).